

Compact Extremely Wideband Antenna with Photonic Crystal Structure Based on MEMS Manufacturing Technology

Xiaoming Zhu^{1, 2, *}, Xiaodong Yang^{1, 3}, and Xiaoguang Wang⁴

Abstract—An extremely wideband photonic crystal antenna is proposed with a very compact size of $16.6 \times 26.6 \times 0.9 \text{ mm}^3$. The double-layer materials of silicon and glass are selected as the antenna substrate. The band gap performance of photonic crystals can decrease electromagnetic wave absorption of silicon substrate, restrain surface wave loss of antenna, and increase electromagnetic wave space radiation. Hence the periodical photonic crystal with square lattices is applied in upper silicon substrate. The glass substrate not only decreases effective dielectric constant of antenna, but also supports silicon substrate with photonic crystal. MEMS processes are used to realize photonic crystal antenna with plenty tiny through-holes. The simulated and measured results demonstrate that photonic crystal can effectively expand the working bandwidth of base antenna.

1. INTRODUCTION

Ultra-wideband (UWB) is a radio engineering technology with very large bandwidth. The ultra-wide frequency range offers several advantages including low power consumption, high data rate, high resolution, resistance to interference, high penetrability, etc. UWB has a wide range of application in high speed communication, image transmission, radar, surveying, positioning and wireless sensor network [1]. Photonic crystal is artificial nonhomogeneous electromagnetic media. The Bragg scattering of electromagnetic waves creates band gaps in photonic crystals. The electromagnetic waves cannot propagate if the frequencies are in the range of photonic band gaps [2]. Traditional antennas usually select low dielectric constant substrates to obtain good radiation performance. There is an inverse relationship between planar size and dielectric constant for antenna design, so traditional antennas are difficult to improve the performance and miniaturization simultaneously. To solve the contradiction relationship, a new type of antenna with photonic crystal structure is designed. In recent several decades, photonic crystals are used in different antennas to enhance performance of bandwidth, gain, radial direction, decoupling, etc. The representative applications include low profile antenna, microstrip antenna, array antenna, slot antenna, high gain antenna and phased-array antenna [3–10]. To realize the special structure of photonic crystal antenna, MEMS is utilized to ensure accurate fabrication. MEMS is a three-dimensional manufacturing technology of micro-electromechanical systems. Fabrication processes include lithography, deposition, oxidation, etching, metallization, bonding, etc. The sequential processes of MEMS can integrate different structures, devices and subsystems as their components in complex multifunctional systems [11–13].

In this letter, an extremely wideband antenna with two-dimensional photonic crystal is proposed. For application in portable wireless devices, the antenna should be small enough and have

Received 19 January 2017, Accepted 8 March 2017, Scheduled 2 May 2017

* Corresponding author: Xiaoming Zhu (zhuxiaoming213@163.com).

¹ College of Information and Communication Engineering, Harbin Engineering University, Harbin 150001, China. ² College of Electrical and Information Engineering, Heilongjiang Institute of Technology, Harbin 150050, China. ³ Collaborative Research Center, Meisei University, Tokyo 1918506, Japan. ⁴ Engineering Center of Chip and Microsystem, 49th Research Institute of CETC, Harbin 150001, China.

omnidirectional radiation. High dielectric constant silicon material is applied as antenna substrate to decrease planar size, but the surface wave loss of silicon base degrades antenna radiation performance. The band gap of photonic crystal can restrain surface wave propagation, so the square lattice photonic crystal is used in silicon antenna to improve bandwidth and radiation performance.

2. ENERGY BAND ANALYSIS OF PHOTONIC CRYSTAL

The photonic crystal structure contains two lattices with the same dimensionality. One is the lattice of real space, and the other is the lattice of reciprocal space [14]. The basis vector of lattice is \mathbf{a}_i , and the basis vector of reciprocal lattice is \mathbf{b}_j . The relationship between them is

$$\mathbf{a}_i \cdot \mathbf{b}_j = 2\pi\delta_{i,j} = \begin{cases} 2\pi & i = j \\ 0 & i \neq j \end{cases} \quad \forall i, j \in [1, N] \quad (1)$$

On the basis of Bloch equation, a point of reciprocal space is regarded as the original point in terms of symmetry of photonic crystal structure. The First Brillouin Zone of photonic crystal consists of the original point and the region bounded by perpendicular bisection plane of proximal points. Based on vectors of reciprocal lattice, all wave vectors can be transformed into the First Brillouin Zone, which is the smallest unit of all Brillouin Zones [15]. The First Brillouin Zone is divided into several equivalent regions according to translational, revolving and mirrored symmetry of photonic crystal. All points are mapped to a smaller region named Irreducible Brillouin Zone, that is surrounded by three boundary points of Γ , X and M . In fact, after the wave vectors of boundary line ($\Gamma \rightarrow X \rightarrow M \rightarrow \Gamma$) are calculated, the energy band dispersion of photonic crystal can be obtained including photonic band gap. If the frequencies are in the photonic band gap area, the electromagnetic waves cannot be transmitted because of total reflection phenomenon in the substrate.

The two-dimensional configuration of photonic crystal is designed into a silicon substrate with regular air holes as shown in Figure 1. The thicknesses of substrate and air holes are both $400 \mu\text{m}$. The lattice period is $a = 1 \text{ mm}$ on behalf of distance between two air holes. The radius of circle air holes is $rad = r1 \times a$, and $r1$ is a scale factor. Figure 1(b) shows the corresponding First Brillouin Zone, where ΓXM region is the Irreducible Brillouin Zone. The coordinate positions of three boundary points are $\Gamma(0, 0)$, $X(\pi/a, 0)$ and $M(\pi/a, \pi/a)$.

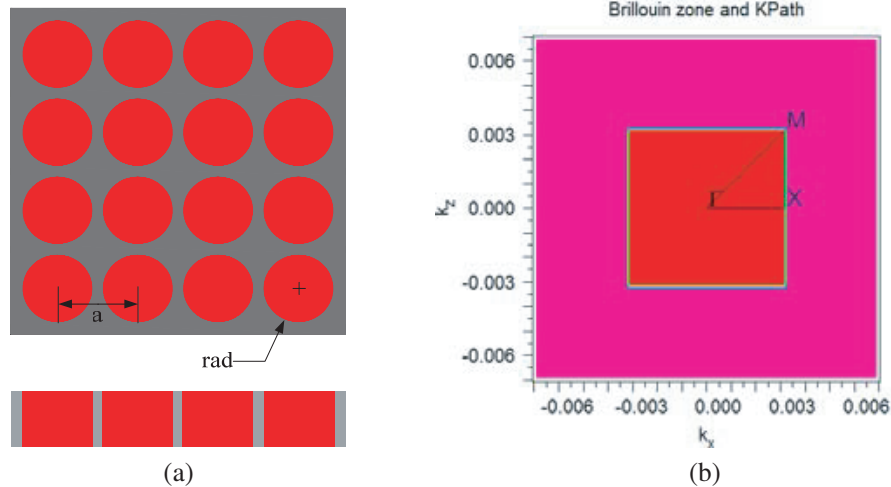


Figure 1. Configuration of photonic crystal with square lattices. (a) The top and side view of photonic crystal. (b) The First Brillouin Zone of photonic crystal.

To obtain wider range of band gap, factor $r1$ is optimized to adjust the radius of air column. When $r1$ is varied from 0.35 to 0.46, the range of band gap is accordingly varied as shown in Figure 2. TE polarized waves are not excited in the silicon substrate, so band gap characteristic is only considered by existent TM waves. The energy band of photonic crystal has three band gaps when $r1$ is varied in

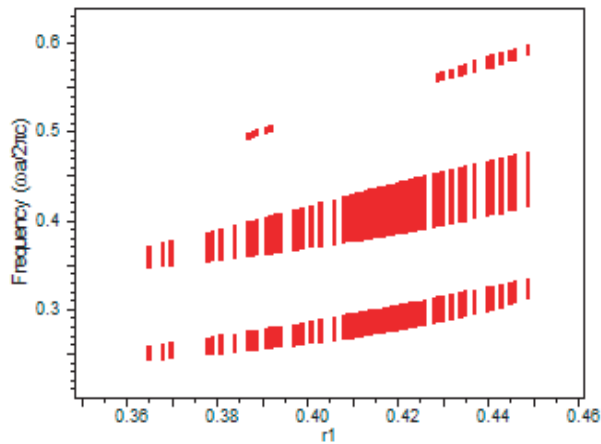


Figure 2. Band gap variation of photonic crystal with different $r1$.

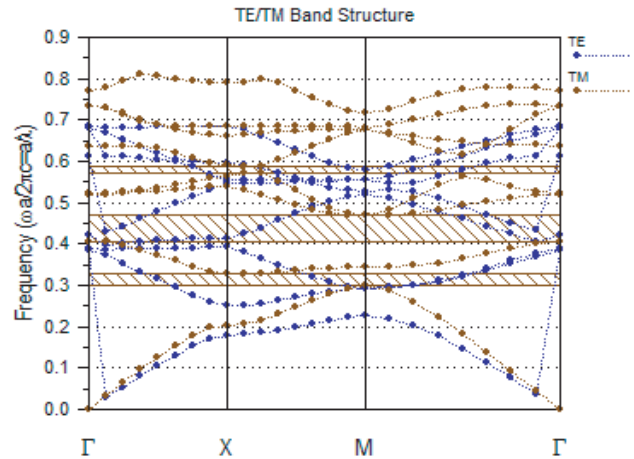


Figure 3. Energy band diagram of photonic crystal with square lattices.

0.438 ~ 0.45. After considering the width of photonic band gap and process realization, $r1$ is designated 0.44 finally. Figure 3 shows the energy band of photonic crystal with air holes radius of 0.44 mm, where horizontal axis represents the wave vector of Irreducible Brillouin Zone, and vertical axis represents normalized frequency. It can be seen that three frequency band gaps of TM waves are 0.299 ~ 0.326, 0.406 ~ 0.467 and 0.572 ~ 0.586. The overall ratio of band gap is 10.2% in the designed photonic crystal with square lattices.

3. DESIGN OF PHOTONIC CRYSTAL ANTENNA

The substrate of photonic crystal antenna is a double-layer structure. The upper layer is silicon material with thickness of 400 μm and relative dielectric constant of 11.9. The lower layer is glass material, whose product model is Pyrex7740, with thickness of 500 μm and relative dielectric constant of 4.6. The silicon and glass can be connected tightly by means of MEMS bonding process. The configuration of photonic crystal antenna is illustrated in Figure 4.

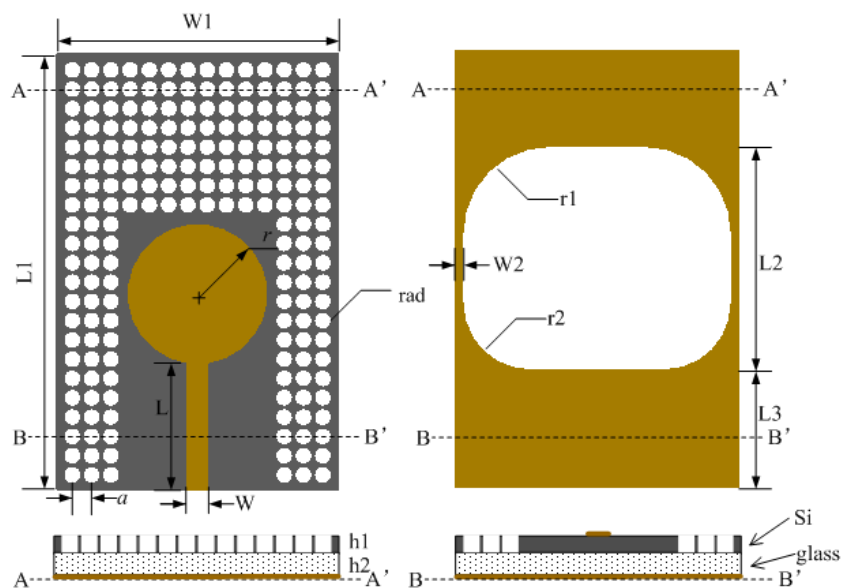


Figure 4. Configuration of photonic crystal antenna with square lattices.

The radiation patch is in classical circular shape, which has better broadband impedance matching than rectangular patch. Meanwhile, the circular patch has small planar size, so more space is left for photonic crystal structure mentioned above. The upper rectangular microstrip line is the feeder used for connecting excitation port and circular patch. The ground plate of microstrip antenna is on the back of the glass substrate with a broad aperture. Four right angles are turned into arc shapes for matching with port impedance of $50\ \Omega$. The square lattices of photonic crystal are designed in the upper silicon layer. The depth of periodic air holes is $400\ \mu\text{m}$, the same as the silicon substrate. The air through-holes are positioned around the radiation patch. The selected parameter values of the proposed antenna are listed in Table 1.

Table 1. Dimensions of the photonic crystal antenna (units: mm).

$W1$	$L1$	r	L	W	$W2$	$L2$
14.6	22.6	3.599	6.637	1.073	0.3811	11.553
$L3$	$r1$	$r2$	$h1$	$h2$	a	rad
6.0793	4.501	3.473	0.4	0.5	1	0.44

The numerical analysis of photonic energy band characteristic is carried out under the condition of photonic crystal with infinite periodic lattices. Superabundant lattices cannot be accepted in practical designing process because of dimensional limit of antenna. On the other hand, a small number of lattice units are unable to form steady photonic band gap performance. Consequently, a balance between antenna dimension and periodic number of square lattice units should be properly decided. Only three rows of lattice units are placed on both sides of the feeder and patch, because antenna and photonic crystal will generate strong mutual coupling to decrease radiation performance of original antenna in close range. The front space of the patch is enough to fit more photonic crystal units.

Additionally, we analyze the impacts of number of lattice rows on return loss of antenna, as shown in Figure 5. When there are six rows of lattice units above circular patch, the role of photonic crystal is obvious. The upper frequency limit of antenna bandwidth is improved from 9.62 GHz to nearly 24 GHz. With the increase of lattice rows, the return loss S_{11} of antenna decreases especially at 7 GHz, 13 GHz and 20 GHz. When the numbers of lattice rows are 8 and 9, the S_{11} curves are almost the same, so there is no need to add rows of photonic crystal. If the antenna has 9 rows of lattice units, some lattices will overlap with circular patch. Because different MEMS processes are applied to the patch of antenna and through-holes of photonic crystal, the overlapping structure will raise MEMS fabrication difficulty. As a result, 8 rows of lattice units are reserved to avoid interaction of two fabrication processes in the entire antenna configuration.

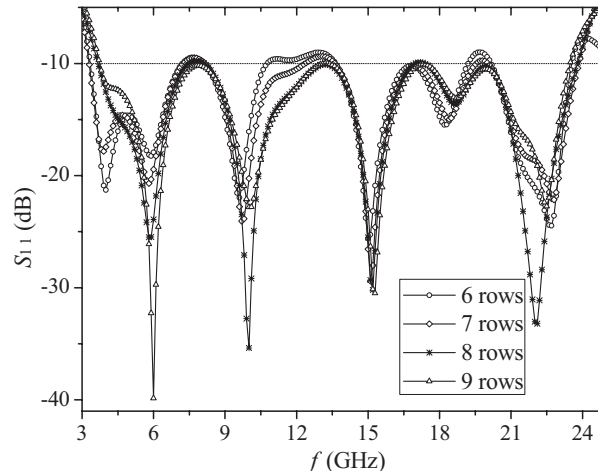


Figure 5. Influence on square lattice photonic crystal antenna with different rows.

4. RESULTS AND DISCUSSION

The proposed photonic crystal antenna is fabricated by MEMS technology. Complete microfabrication processes with integrated sequential processes are of great importance. The main process flowchart is given in Figure 6. The figures of patch and ground are formed by photolithography technique. ICP etching process is adopted to produce numerous air through-holes in silicon substrate. The bonding process can realize connection of silicon and glass without any binder. Based on above MEMS processes, the photonic crystal antenna is obtained, as shown in Figure 7.

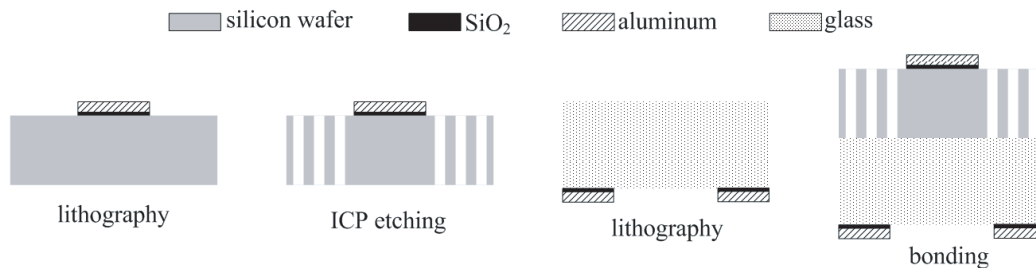


Figure 6. Schematic description of the process steps used to fabricate photonic crystal antenna.

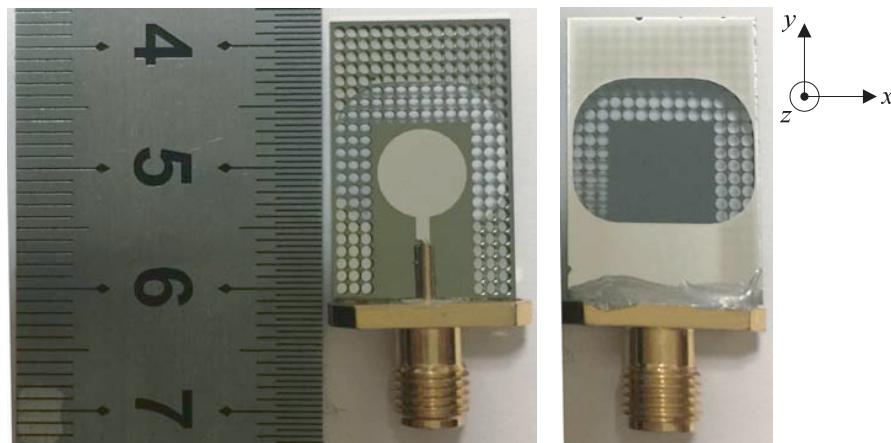


Figure 7. Photograph of the fabricated photonic crystal antenna.

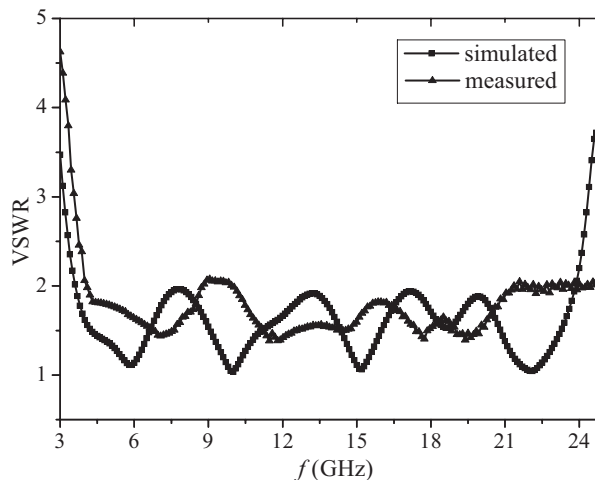


Figure 8. Simulated and measured VSWR of photonic crystal antenna.

The simulated and measured VSWR curves of this antenna are illustrated in Figure 8. The simulated result of antenna displays extremely wideband performance in the frequency ranges of 3.64 ~ 23.8 GHz. The measured VSWR nearly agrees well with the simulated one, except that lower frequency limit of antenna is 3.9 GHz, which is a little higher than simulated frequency. The bandwidth of the base antenna is increased from 6 GHz to 20 GHz by means of adding square lattice photonic crystal. It is indicated that photonic crystal structure can take advantage of photonic band gap characteristic to enhance antenna bandwidth obviously.

The measured radiation patterns are shown in Figure 9 at 4 GHz, 8 GHz, 12 GHz and 18 GHz. The pattern displays two nulls satisfied with characteristic of dipole antenna in yz plane. The radiation pattern generates little fluctuation in high frequencies, but the omnidirectional radiation performance can be seen in xz plane.

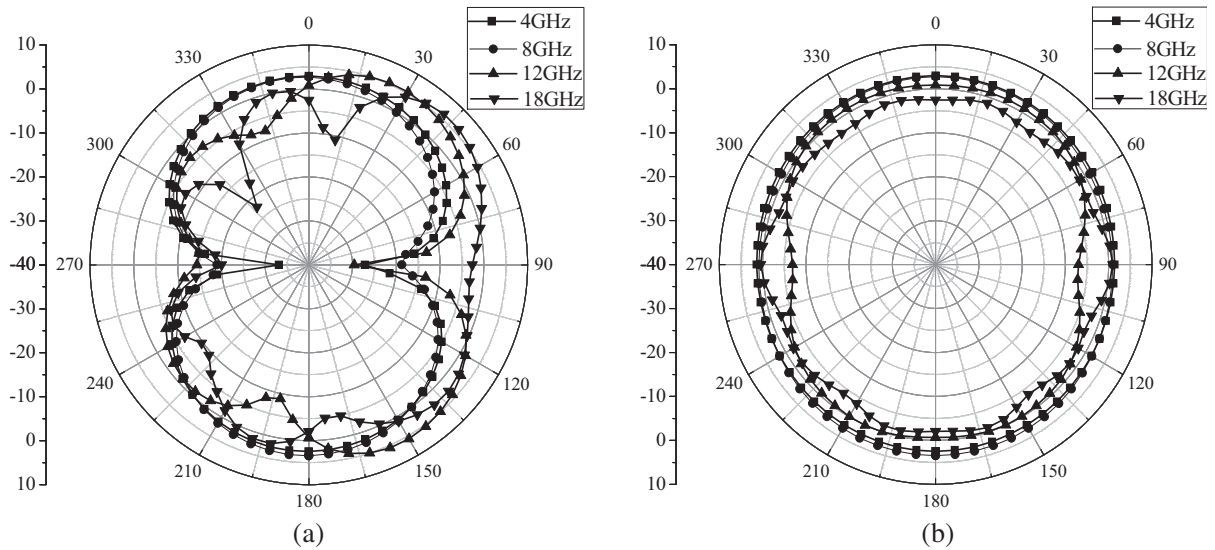


Figure 9. Radiation patterns of photonic crystal antennas. (a) yz plane. (b) xz plane.

5. CONCLUSIONS

The application of photonic crystal is researched in antenna designing. The photonic band gap characteristic is able to restrain surface wave loss of antenna substrate with high dielectric constant and improve bandwidth and radiation performance of the proposed antenna. MEMS technology is utilized to manufacture photonic crystal antenna. The proposed antenna has not only very compact planar dimension, but also an extremely wide working bandwidth from 3.9 GHz to 23.8 GHz. The next research will focus on more photonic crystal structures to enhance different radiation performances of antennas.

REFERENCES

1. Federal Communications Commission (FCC), "First report and order in the matter of revision of Part 15 of the commission's rules regarding ultra-wideband transmission systems," ET-Docket, 98-153, 2002.
2. Joannopoulos, J. D., R. D. Meade, and J. N. Winn, *Photonic Crystal: Molding the Flow of Light*, 3-5, Princeton University Press, Princeton, 1995.
3. Pereira Jonathan, P. P., P. Da Silva José, and G. O. De Ádller, "Microstrip antennas design based in periodic and quasiperiodic PBG symmetries," *Microwave and Optical Technology Letters*, Vol. 57, No. 12, 2914-2917, 2015.

4. Leger, L., T. Monediere, and B. Jecko, "Enhancement of gain and radiation bandwidth for a planar 1-D EBG antenna," *IEEE Microwave Wireless Communication Letter*, Vol. 15, No. 9, 573–575, 2005.
5. Zeb, B. A., K. P. Esselle, and R. M. Hashmi, "Computational models for bandwidth enhancement of electromagnetic bandgap (EBG) resonator antennas and their limitations," *IEEE International Conference on Computational Electromagnetics*, 19–21, 2015.
6. Neumann, N., R. Trieb, W.-S. Benedix, and D. Plettemeier, "Active integrated photonic antenna array," *Proceedings of the 2012 IEEE-APS Topical Conference on Antennas and Propagation in Wireless Communications*, 648–651, 2012.
7. Panda, P. K. and D. Ghosh, "Mushroom-like EBG structures for reducing RCS of patch antenna arrays," *International Conference on Microwave and Photonics*, 2013.
8. Cheype, C., C. Serier, and M. Thèvenot, "An electromagnetic bandgap resonator antenna," *IEEE Transactions on Antennas and Propagation*, Vol. 50, No. 9, 1285–1290, 2002.
9. Weily, A. R., L. Horvath, and K. P. Esselle, "A planar resonator antenna based on a woodpile EBG material," *IEEE Transactions on Antennas and Propagation*, Vol. 53, No. 1, 216–223, 2005.
10. Liu, W., Z. N. Chen, and X. Qing, "60-GHz thin broadband high-gain LTCC metamaterial-mushroom antenna array," *IEEE Transactions on Antennas and Propagation*, Vol. 62, No. 9, 4592–4601, 2014.
11. Seassal, C., C. Monat, J. Mouette, et al., "InP bonded membrane photonics components and circuits: Toward 2.5 dimensional micro-nano-photonics," *IEEE Journal of Selected Topics in Quantum Electronic*, Vol. 11, No. 2, 395–407, 2005.
12. Hattori, H. T., C. Seassal, X. Letartre, et al., "Coupling analysis of heterogeneous integrated InP based photonic crystal triangular lattice band-edge lasers and silicon waveguides," *Optics Express*, Vol. 13, No. 9, 3310–3322, 2005.
13. Oliver, J. M., J.-M. Rollin, K. Vanhille, et al., "A W-band micromachined 3-D cavity-backed patch antenna array with integrated diode detector," *IEEE Transactions on Microwave Theory and Techniques*, Vol. 60, No. 2, 284–292, 2012.
14. Prather, D. W., S. Shi, A. Sharkawy, J. Murakowski, and G. J. Schneider, *Photonic Crystals: Theory, Applications, and Fabrication*, 562–590, Wiley, Hoboken, N.J., 2009.
15. Sibilina, C., *Photonic Crystals: Physics and Technology*, 223–243, Springer, Milano, 2008.